

## Optically forbidden excitations of the 3s subshell in the 3d transition metals by inelastic scattering of fast electrons

L. A. Grunes and R. D. Leapman

*School of Applied and Engineering Physics and the Materials Science Center,  
Cornell University, Ithaca, New York 14853*

(Received 21 January 1980)

Electron-energy-loss spectra of 75-keV electrons have been recorded from thin evaporated films of the 3d transition metals. Spectra have been measured in the region of the 3s subshell excitation ( $M_1$  edge) at different momentum transfers. At small  $q$ , no significant intensity at the  $M_1$  threshold is found, but at larger  $q$  ( $\geq 1 \text{ \AA}^{-1}$ ), weak but sharp peaks are observed. These are attributed to the optically forbidden  $3s \rightarrow 3d$  transitions. Widths of these peaks for the metals titanium, chromium, iron, and nickel and their oxides  $\text{TiO}_2$ ,  $\text{Cr}_2\text{O}_3$ , and  $\text{NiO}$  are measured and compared with both the expected widths for the unoccupied portions of the 3d bands and the intrinsic  $M_1$  core level widths.

### I. INTRODUCTION

For small scattering angles or momentum transfers the cross section for inelastic electron scattering, within the single-particle model, for excitation of a core electron from an initial state  $|i\rangle$  to a final state  $|f\rangle$  is given in terms of a dipole matrix element. In this limit, optical selection rules apply and the change in angular momentum must be  $\pm 1$ . However, when the transferred momentum,  $\hbar q$ , is not small, dipole forbidden transitions can occur. The first-row transition metals, with their strongly peaked 3d bands, are ideally suited for observation of optically forbidden  $3s$  to  $3d$  transitions ( $\Delta l = \pm 2$ ). Work has already been reported by Meixner *et al.*<sup>1</sup> showing that transitions to 3d states from the 3s subshell in nickel are observed at large momentum transfers but not at  $q \cong 0$ . This seems to be the only measurement of this type in the literature using inelastic scattering of fast electrons. Misell and Atkins<sup>2</sup> have measured  $M_1$  edges in vanadium and chromium, but these spectra were integrated over a large angular range and the  $q$  dependence was not studied. We have therefore decided to extend measurements to other 3d transition metals in order to investigate systematically the behavior through the period.

First, we estimate the magnitude of  $q$  required to observe dipole forbidden transitions. For electron scattering, the cross-section differential with respect to energy loss  $E$  and solid angle  $\Omega$  is given by<sup>3</sup>

$$\frac{d^2\sigma_{if}}{dEd\Omega}(\vec{q}, E) = \frac{4}{a_0^2 q^4} |\langle f | \exp(i\vec{q} \cdot \vec{r}) | i \rangle|^2, \quad (1)$$

where  $\vec{q}$  is the momentum transfer and  $a_0$  is the Bohr radius. The momentum transfer is related to the scattering angle  $\theta$  and the incident electron momentum  $k$  by  $q^2 = k^2(\theta^2 + \theta_E^2)$ , where  $\theta_E = mE/\hbar^2 k^2$ . For the scattering angles we shall be

considering,  $\theta \gg \theta_E$  hence  $q \approx q_{\perp} = k\theta$ , and the momentum transfer is perpendicular to the incident beam. In the limit  $q \ll 1/r_c$ , where  $r_c$  is the characteristic core wave-function radius, the exponential in Eq. (1) may be expanded to give

$$\begin{aligned} & \frac{d^2\sigma_{if}}{dEd\Omega}(\vec{q}, E) \\ &= \frac{4}{a_0^2 q^4} |\langle f | 1 + iq(\hat{\epsilon}_q \cdot \vec{r}) - \frac{q^2}{2}(\hat{\epsilon}_q \cdot \vec{r})^2 + \dots | i \rangle|^2 \end{aligned} \quad (2)$$

with  $\hat{\epsilon}_q$  a unit vector along  $\vec{q}$ . The first term in the matrix element vanishes because of the orthogonality of states with different energies. Next comes the dipole term, which dominates at small  $\vec{q}$ , and is the source of the optical ( $\Delta l = \pm 1$ ) transitions observed in x-ray absorption spectroscopy. This contribution to the cross section falls off as  $1/q^2$ ; hence at large momentum transfers, the third term (which has no dependence on the magnitude of  $\vec{q}$ ) becomes important, giving rise to monopole ( $\Delta l = 0$ ) and quadrupole ( $\Delta l = \pm 2$ ) transitions.<sup>4</sup> Therefore, in order to observe  $3s \rightarrow 3d$  transitions, we must look for electrons scattered to sufficiently large angles so that the approximation of the matrix element by the dipole term is invalid. This will certainly occur when  $q \approx 1/r_c$ . For the chromium 3s wave function, half the charge density lies within  $r_c \cong 0.4 \text{ \AA}$ .<sup>5</sup> It follows that we may expect to observe optically forbidden transitions at momentum transfers of order  $2.5 \text{ \AA}^{-1}$ , although they should still be observable at somewhat smaller  $q$ . The probabilities for the transitions will be relatively weak, but it is nonetheless reasonable to measure intensity at these scattering angles. Background intensity from the Bragg-diffracted beams generally occurs at somewhat larger  $q$ , e.g.,  $3.1 \text{ \AA}^{-1}$  in chromium.

## II. EXPERIMENTAL

Thin metallic films were prepared by electron-beam evaporation in a Varian high-vacuum system at a pressure of about  $10^{-7}$  torr. Film thicknesses of 150-Å titanium, 150-Å chromium, 260-Å iron, 90-Å nickel, and 240-Å copper were measured using a quartz-crystal thickness monitor situated near the substrate, which was the (100) face of a rock-salt crystal. All the films obtained in this way were polycrystalline with a grain size between 100 and 1000 Å. They were floated off in ethanol and supported on 400-mesh 3-mm diameter copper grids. In the case of titanium, which was very reactive, it was found necessary to protect the film against oxidation by evaporating 40 Å of chromium on either side of the titanium. The metal films were transferred to the vacuum of the electron microscope as quickly as possible. The films were characterized by means of electron diffraction before and after spectra were recorded. All the diffraction patterns agreed with the  $d$  spacings as given by the x-ray powder diffraction file, and the metals did not show appreciable extra rings due to oxidation. It was found that the chromium evaporated onto the titanium did not show up in the diffraction rings and it seems probable that alloying occurred. However, titanium rings were present and the chromium was apparently successful in preventing oxidation.

The experimental system for recording the spectra has been previously described.<sup>6</sup> This consists of an HU-11A electron microscope combined with a retarding-field Wien filter spectrometer. Using the electron microscope in the selected area diffraction mode, a 4- $\mu$ m spot of 75-keV electrons is incident on the specimen with a beam divergence of less than  $10^{-3}$  rad. An entrance slit to the Wien filter spectrometer selects electrons according to their scattering angle, and the spectrometer disperses them in a direction perpendicular to the slit. A two-dimensional pattern results, giving a map of the scattered electron intensity as a function of energy loss and scattering angle. The intensity can be recorded in parallel on photographic plates. Alternatively, accurate digital spectra can be obtained by scanning the energy loss across an aperture and counting single pulses from a scintillator-photomultiplier tube. These operations are controlled by a microcomputer,<sup>7</sup> which also stores and displays the spectrum. After acquisition, the data are uploaded to a larger PDP 11 computer<sup>8</sup> for processing.

Absolute measurement of the energy losses was accurate to about 0.5 eV and the energy resolution varied between 0.8 and 1.5 eV depending on the filament heater current. Angular calibration was carried out using the polycrystalline ring diffraction pattern. Different angles or momentum transfers for recording the digital energy scans could be selected by de-

flecting the pattern by a known amount so that only electrons at these angles reached the scintillator.

## III. RESULTS

Figure 1(a) shows a digital scan of the energy-loss spectrum of chromium from 0 to 100 eV at zero momentum transfer. Three main features occur in this energy range. The weak peak at 11 eV and the strong broad peak at 25 eV are both attributed to plasmon excitations.<sup>2</sup> The intensity rise at 43 eV corresponds to the onset of the  $M_{23}$  edge (excitation of  $3p$  electrons). It is noted that the shape of the spectrum is similar to the single scattering profile obtained by Misell and Atkins.<sup>2</sup> We may conclude that multiple inelastic scattering is relatively small for the 150-Å chromium film. Since in the present work we are looking for weak peaks in the spectrum, it is essential that multiple scattering, which can give spurious structure, should be kept to a minimum.

Figure 1(b) shows a digital scan of the energy-loss spectrum in the region of the  $M$ -shell excitation for chromium at both small and large momentum transfers ( $q_{\perp} = 0.50 \text{ \AA}^{-1}$  and  $2.20 \text{ \AA}^{-1}$ , respectively). The shape of the  $M_{23}$  edge has been described in terms of a Fano interference effect between transitions to the empty  $3d$  band and excitations of the  $3d$  electrons to states in the  $f$  continuum.<sup>9</sup> This interference effect gives rise to a completely different spectrum compared with that of  $2p$  excitations, for example.<sup>10</sup> These  $M_{23}$  edges were observed in all the transition-metal films examined, but we are not concerned with them here; instead we concentrate on the weak  $M_1$  peak which shows up on the tail of the  $M_{23}$  edge at large  $q$  but not at  $q_{\perp} \rightarrow 0$ . This may be attributed to the  $3s \rightarrow 3d$  band excitation. Figure 2 shows on a suitably expanded scale digital energy-loss scans in the region of the  $M_1$  edge for titanium, chromium, iron, nickel, and copper, respectively. Although the visibility varies from element to element, a clear peak is observed in all cases except for copper. (The vertical intensity scales have been shifted arbitrarily.)

Table I lists the  $M_1$  energies as measured at the half height of the peak obtained after the background subtraction described below. These are compared with the electron binding-energy data of Siegbahn *et al.*<sup>11</sup> and are found to agree within 2 eV. We estimate an accuracy of about  $\pm 1$  eV in our measurements. Also listed in Table I are results on oxide films of  $\text{TiO}_2$ ,  $\text{Cr}_2\text{O}_3$ , and  $\text{NiO}$ . These were prepared by heating in air metal films already supported on grids. The oxides were characterized by their ring diffraction patterns as was done for the metals. We note a shift up in energy of 4 eV in the case of  $\text{TiO}_2$  compared to titanium. Such a shift is to be expected because of the change in chemical environment of the titanium atom. For example, the  $L_{23}$  edge ( $2p$

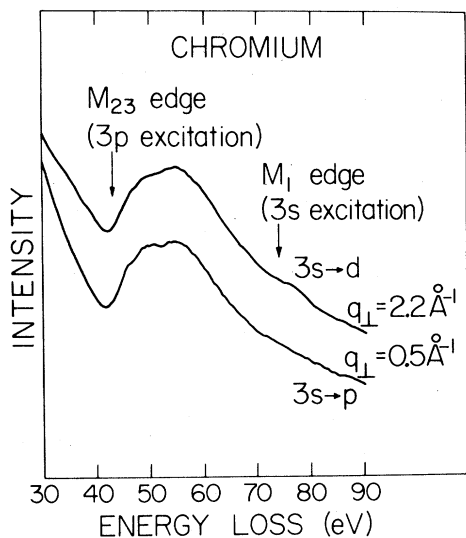
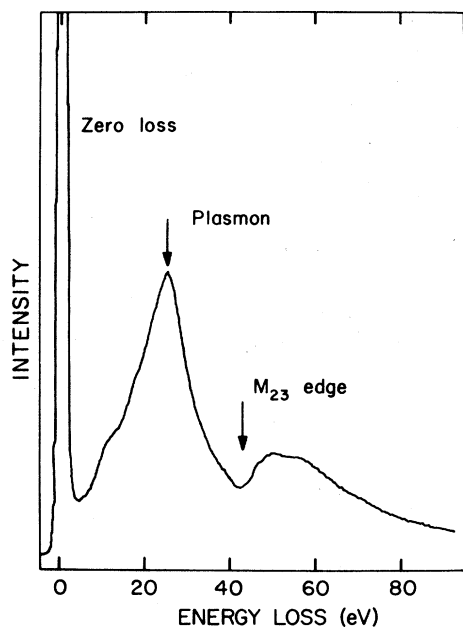


FIG. 1. (a) Energy-loss spectra at  $q_{\perp}=0$  of a 150-Å chromium film showing plasmon excitations of the valence electrons and the  $3p$  core excitation. (b) Enlarged spectra showing  $M_1$  edge at large  $q$  but not at small  $q$ . Absolute intensities are not scaled to one another.

excitation) in  $\text{TiO}_2$  is found to be shifted up in energy by 2 eV from titanium both in our electron-energy-loss measurements<sup>12</sup> and in x-ray absorption studies by Fischer.<sup>13</sup> The apparently larger shift for the  $M_1$  edge might be expected since the  $3s$  core level has a much smaller binding energy than the  $2p$  level and hence is more likely to be affected by the chemical environment. We find no significant shift in  $M_1$

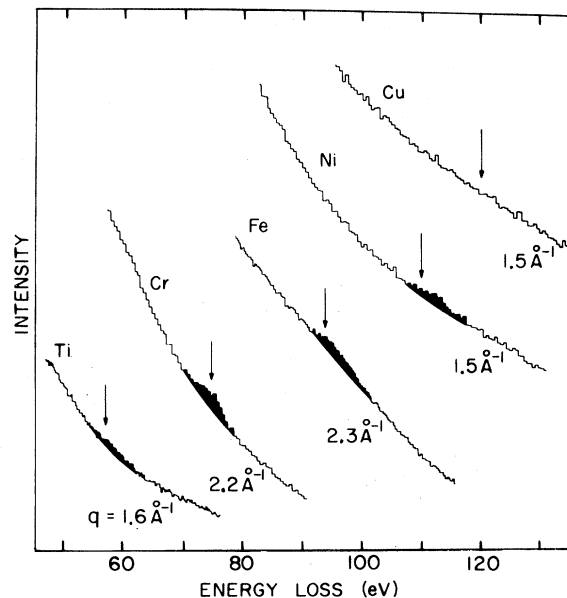


FIG. 2. Spectra at large  $q$  in the region of the  $3s$  shell excitation for elements in the  $3d$  transition series. The vertical scales have been arbitrarily displaced for convenience.

energy, within our accuracy of  $\pm 1$  eV, for  $\text{Cr}_2\text{O}_3$  and  $\text{NiO}$  compared with the metals. Table I also lists the  $M_1$  full width at half maximum (FWHM) for each sample. The corrected values, after Gaussian quadrature subtraction of the incident beam width, are shown adjacent to the measured widths [corrected width =  $[(\text{measured width})^2 - (\text{incident beam width})^2]^{1/2}$ ]. The widths were measured by fitting a background intensity before and after the peak to a cubic polynomial. A justification for this procedure is that the feature of interest at the  $M_1$  edge consists of a fairly narrow peak of width a few eV. A polynomial fit was chosen since the underlying intensity, consisting mainly of the tail of the  $M_{23}$  edge, is comparatively slowly varying and does not have a simple form. Other expressions for the background fit were not found to be useful, e.g., an inverse power law  $E^{-r}$ , which holds at large energy losses.<sup>14</sup>

Figure 3 shows the chromium  $M_1$  peak with the background subtracted in this fashion from the spectrum in Fig. 2. The measured width in this case is 4.5 eV. The widths for the other metals vary from 4.0 eV in titanium to 6.5 eV in iron. The widths of the  $M_1$  peaks in the oxides are seen to be systematically narrower than the respective metals.

We note in Fig. 1(b) that at large  $q$  the  $M_{23}$  edge is still visible and has a similar shape to that at small  $q$ . The  $1/q^2$  dependence of the dipole matrix element term in Eq. (2) would dictate that the  $M_{23}$  intensity at  $2.2 \text{ \AA}^{-1}$  be a factor of  $\sim 20$  down from that seen at  $0.5 \text{ \AA}^{-1}$ . We measure on a photographic plate (paral-

TABLE I. Full widths at half maxima and energies in eV for excitation of the 3s core level. The second column has been corrected for the energy width of the incident beam. Uncertainties for the widths are  $\pm 0.5$  eV for the metals and  $\pm 1$  eV for the oxides. The energy position measurements are all accurate to  $\pm 1$  eV, and the 3s binding energies are from Siegbahn *et al.* (Ref. 11).

Sample	Measured $M_1$ FWHM	Corrected $M_1$ FWHM	$M_1$ energy	3s binding energy
Ti	4.0	3.7	57	59
TiO <sub>2</sub>	3.0	2.6	61	
Cr	4.5	4.1	75	74
Cr <sub>2</sub> O <sub>3</sub>	4.0	3.6	74	
Fe	6.5	6.4	94	95
Ni	4.6	4.4	110	112
NiO	2.7	2.3	109	

lel recording) a ratio of only  $\sim 8$ . Our larger than expected  $M_{23}$  intensity at large  $q$  can be attributed to multiple elastic and quasielastic (phonon and static defects) scattering: the very strong intensity of the  $M_{23}$  edge at  $q_1 \rightarrow 0$  is rescattered to higher angles and is superimposed on the much weaker single scattering intensity. The peak we observe at the  $M_1$  edge, how-

ever, cannot be attributed to multiple scattering. If this were the case, it would also be seen at  $q_1 = 0$ . Also, we note that no combination of the volume and surface plasmons and the  $M_{23}$  edge gives an excitation of an energy that might be mistaken for an  $M_1$  peak. Since the bulk plasmon and  $M_{23}$  edge both have energy widths considerably wider than the feature observed, we conclude that our identification of the  $M_1$  peak is correct.

The  $q$  dependence of the  $M_1$  peak in chromium was measured from a spectrum recorded on a photographic plate as a function of scattering angle. Densitometer traces across the edge were measured at different  $q$  values extending out towards the first Bragg ring ( $3.1 \text{ \AA}^{-1}$ ). The  $M_1$  intensity was estimated by subtracting the extrapolated background intensity. Results are shown in Fig. 4. The intensity is approximately constant as a function of  $q$  as expected from the  $q^2$  term in the matrix element responsible for the

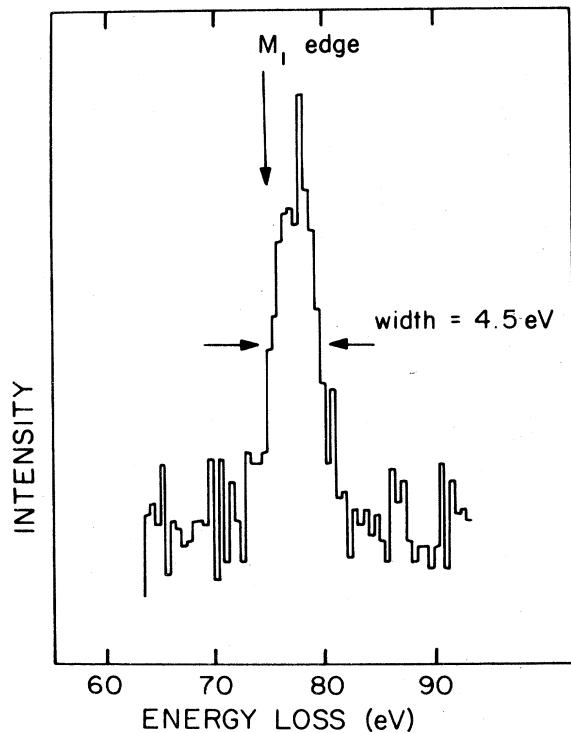


FIG. 3.  $M_1$  intensity for chromium after background subtraction.

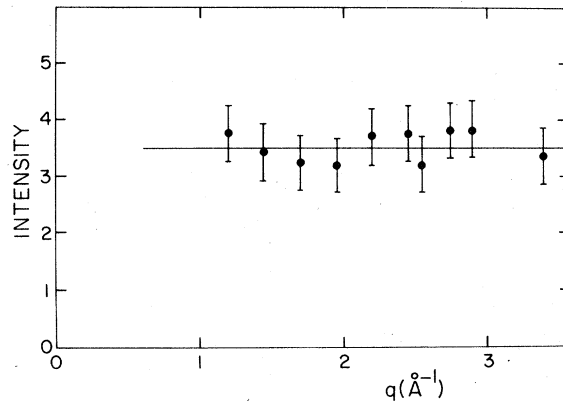


FIG. 4. Intensity of the chromium  $M_1$  peak as measured from a photographic plate plotted as a function of momentum transfer.

optically forbidden transitions

$$\frac{d^2\sigma_{if}(\vec{q}, E)}{dE d\Omega} \propto \frac{|\langle f | (\vec{q} \cdot \vec{r})^2 | i \rangle|^2}{q^4}$$

$$\propto |\langle f | (\hat{\epsilon}_q \cdot \vec{r})^2 | i \rangle|^2 = \text{constant} \quad (3)$$

The photographic plate is very convenient for making this type of measurement, since the data are recorded in parallel; hence we need not normalize the intensities with respect to the incident beam.

#### IV. CONCLUSIONS AND DISCUSSION

The above results show that peaks are found in the spectrum at energies which agree well with the binding energies for the  $M_1$  levels as determined by photoemission measurements.<sup>11</sup> Their occurrence at large  $q$  but not at small  $q$  indicates that they arise from optically forbidden transitions. This work extends the results of Meixner *et al.*,<sup>1</sup> who observed these optically forbidden transitions in nickel.

It is interesting to note that another type of nondipole transition is evident at large momentum transfers in electron-energy-loss spectra. This arises when electrons are excited to energies far above the Fermi level such that the energy transferred is much greater than the core binding energy. The scattered intensity is then peaked at an angle  $\theta_c = (E/E_0)^{1/2}$ , where  $E_0$  is the incident electron energy. Classically, the collisions may be considered as "close" rather than "glancing," and we expect a peak at this angle through conservation of energy and momentum. This effect is known as the Bethe ridge<sup>15</sup> and is associated with large changes in angular momentum so that higher terms than the quadrupole one are involved in the matrix element. The Bethe ridge has been observed, for example, in the excitation of  $2s$  and  $2p$  electrons in energy-loss spectra from carbon films.<sup>14</sup> The optically forbidden transitions which we consider in the present work have been shown by their momentum-transfer dependence to correspond to the quadrupole term in the matrix element. Such behavior was found not only for chromium as described above, but also for the other materials studied. This is as expected on the basis of  $3s \rightarrow 3d$  transitions, which are observable because the density of unoccupied states above the Fermi level is large in the  $3d$  transition metals. The fact that no peak was observed in the case of copper, which has a filled  $3d$  band, supports this interpretation.

In subtracting the background intensity underlying the  $M_1$  edge, we have assumed that other contributions from the  $3s$ -shell excitation are small at energies near threshold. The subtracted peak does not represent the total  $M_1$  intensity, but rather separates out the contribution due to the  $3s \rightarrow 3d$  band transitions. Calculations of the total conduction-band density of states<sup>16</sup> show that the contribution from the

TABLE II. Comparison in eV of the full widths at half maxima for excitation of the  $2p$  level with the width of the unoccupied  $3d$  band as calculated by Müller and Wilkins (Ref. 16).

Sample	Corrected $L_3$ FWHM	Calculated $3d$ -band width
Ti	4.6	2.9
TiO <sub>2</sub>	4.0	
Cr	4.3	2.6
Cr <sub>2</sub> O <sub>3</sub>	3.2	
Fe	3.5	0.7
Ni	3.0	0.1
NiO	1.2	

narrow  $3d$  band is by far the strongest. Also spectra due to excitation of  $2p$  electrons in the  $3d$  transition metals reveal intense "white lines" attributed to these high-density  $d$  states.<sup>10,12,17</sup>

The width of the unoccupied  $3d$  bands as determined by band calculations<sup>16</sup> shows a decreasing trend with increasing atomic number for these elements as seen in Table II. This trend is also evident in our<sup>12</sup> measured widths of the  $L_3$  edges ( $2p - 3d$  excitations), which are shown in the next column of the table. For titanium and chromium, the widths of the  $M_1$  peaks in Table I are approximately equal (about 4 eV) to the  $L_3$  linewidths. These are larger by about 1 eV than the calculated  $d$ -band widths. In the case of iron and nickel, the  $M_1$  widths are significantly larger than both the  $L_3$  widths and those of the calculated density of states. The larger than expected width of the  $M_1$  peaks in these metals can be at least partially accounted for by core hole effects. An intrinsic energy width due to the  $3s$  hole lifetime has been calculated by Yin *et al.*<sup>18</sup> These authors find the width increases through the  $3d$  transition period, ranging from 1.2 eV in titanium to 1.8 eV in nickel. Their experimentally determined values (for copper and zinc) using x-ray photoemission are consistent with this theory. McGuire<sup>19</sup> calculates a similar increasing trend in  $3s$  core width with atomic number, although the values are larger. In both calculations, the increasing  $M_1$  core width is attributed to an increasing probability of Coster-Kronig and super Coster-Kronig de-excitation transitions. A further explanation for our large observed  $M_1$  width in iron is that the  $3s$  level is split by an exchange interaction with the five unpaired  $3d$  valence electrons. Fadley and Shirley<sup>20</sup> find from photoemission experiments that the  $M_1$  level in iron is split into two components separated by 4.4 eV. This effect is expected to be more pronounced at the middle of the period where there are more unpaired valence electrons.

For the oxides the widths of both the  $M_1$  and the  $L_3$  peaks are systematically narrower than in the respective metals. This is consistent with a narrower width of the unoccupied 3d states in the oxides. A more complete discussion of the  $L_{23}$  excitations in both the metals and the oxides will be included in a forthcoming paper.

#### ACKNOWLEDGMENTS

We wish to thank Professor J. Silcox, Dr. J. E. Müller, Dr. P. E. Batson, and A. B. Ray for helpful discussions. Financial support from the National Science Foundation through the Cornell University Materials Science Center is gratefully acknowledged.

- <sup>1</sup>A. E. Meixner, R. E. Dietz, G. S. Brown, and P. M. Platzman, *Solid State Commun.* **27**, 1255 (1978).
- <sup>2</sup>D. L. Misell and A. J. Atkins, *Philos. Mag.* **27**, 95 (1973).
- <sup>3</sup>H. A. Bethe, *Ann. Phys. (Leipzig)* **5**, 325 (1930).
- <sup>4</sup>J. J. Ritsko, N. O. Lipari, P. C. Gibbons, S. E. Schnatterly, J. R. Fields, and R. Devaty, *Phys. Rev. Lett.* **36**, 210 (1976).
- <sup>5</sup>See F. Herman and S. Skillman, *Atomic Structure Calculations* (Prentice-Hall, Englewood Cliffs, 1963).
- <sup>6</sup>G. H. Curtis and J. Silcox, *Rev. Sci. Instrum.* **42**, 630 (1971).
- <sup>7</sup>B. Watkins and P. L. Fejes, available in Proceedings of the Cornell Analytical Electron Microscopy Workshop, 1978, from Cornell Materials Science Center (MSC Report No. 3082) (unpublished).
- <sup>8</sup>P. E. Batson, Ph.D. thesis (Cornell University, 1976) (unpublished); P. E. Batson, J. Silcox, and R. Vincent, in *Proceedings of the 29th Annual Meeting of the Electron Microscopy Society of America, Boston, 1971*, edited by C. J. Arcenaux (Claitor, Baton Rouge, 1971), p. 30.
- <sup>9</sup>L. C. Davis and L. A. Feldkamp, *Solid State Commun.* **19**, 413 (1976).
- <sup>10</sup>B. Brousseau-Lahaye, C. Colliex, J. Frandon, M. Gasgnier, and P. Trebbia, *Phys. Status Solidi B* **69**, 257 (1975).
- <sup>11</sup>K. Siegbahn, C. Nording, A. Fahlman, R. Nordberg, K. Homrin, J. Hedman, G. Johansson, T. Bergmark, S. Karlsson, I. Lindgren, and B. Lindberg, *Nova Acta Regiae Soc. Sci. Ups. Ser. IV* **20**, 224 (1967).
- <sup>12</sup>R. D. Leapman and L. A. Grunes (unpublished).
- <sup>13</sup>D. W. Fischer, *Phys. Rev. B* **5**, 4219 (1972).
- <sup>14</sup>R. F. Egerton, *Philos. Mag.* **31**, 199 (1971).
- <sup>15</sup>M. Inokuti, *Rev. Mod. Phys.* **43**, 297 (1971).
- <sup>16</sup>J. E. Müller and J. W. Wilkins (unpublished); J. E. Müller, Ph.D. thesis (Cornell University, 1980) (unpublished).
- <sup>17</sup>C. Bonnelle, *Ann. Phys. (Paris)* **1**, 439 (1966).
- <sup>18</sup>L. I. Yin, I. Adler, T. Tsang, M. H. Chen, D. A. Ringers, and B. W. Crasemann, *Phys. Rev. A* **9**, 1070 (1974); **17**, 1556 (1978).
- <sup>19</sup>E. J. McGuire, *Phys. Rev. A* **5**, 1043 (1972).
- <sup>20</sup>S. Fadley and D. A. Shirley, *Phys. Rev. A* **2**, 1109 (1970).